

# Corrosion study of steels exposed over five years to the humid tropical atmosphere of Panama

Juan A. Jaén<sup>1</sup>  · Josefina Iglesias<sup>2</sup>

© Springer International Publishing Switzerland 2017

**Abstract** The results of assessing five-year corrosion of low-carbon and conventional weathering steels exposed to the Panamanian tropical atmosphere is presented. Two different test sites, one in Panama City: 5 km from the shoreline of the Pacific Ocean, and another in the marine environment of Fort Sherman, Caribbean coast of Panama; namely, Fort Sherman Coastal site: 100 m from coastline. The corrosion products, formed in the skyward and earthward faces in the studied tropical environment, were mainly identified using room temperature and low temperature (15 K) Mössbauer spectroscopy, and ATR-FTIR. In all samples, lepidocrocite ( $\gamma$ -FeOOH) and goethite ( $\alpha$ -FeOOH) were the main constituents. Some maghemite ( $\gamma$ -Fe<sub>2</sub>O<sub>3</sub>), was also identified in Tocumen by Mössbauer spectroscopy and traces of ferroxhyte ( $\delta$ -FeOOH) using ATR-FTIR. The corrosion rate values obtained are discussed in light of the atmospheric exposure conditions and atmospheric pollutants.

**Keywords** Mild carbon steel · Weathering steel · Atmospheric corrosion · Mössbauer spectroscopy · ATR-FTIR

---

This article is part of the Topical Collection on *Proceedings of the 15th Latin American Conference on the Applications of the Mössbauer Effect (LACAME 2016), 13–18 November 2016, Panama City, Panama*  
Edited by Juan A. Jaén

---

✉ Juan A. Jaén  
juan.jaen@up.ac.pa

<sup>1</sup> Departamento de Química Física, Edificio de Laboratorios Científicos-VIP, Universidad de Panamá, Panamá, Panamá

<sup>2</sup> Laboratorio de Análisis Industriales y Ciencias Ambientales, Universidad Tecnológica de Panamá, Panamá, Panamá

## 1 Introduction

Mild carbon steel (MCS) and weathering steel (WS) can be maintained for prolonged time exposure to the environment at low cost and without coating. Different types of steels corrode at rates determined by the environment. Weathering steels exhibit enhanced corrosion resistance attributed to the formation of a patina, a tightly adherent protective rust layers. The protective properties of the patina depend on the chemical composition of metal, the humid–dry cycles, pH, composition of rainwater and atmospheric pollutants [1]. Therefore, it is important to study the corrosion parameters and their role in the formation of rust products during the period of exposure.

Corrosion in marine tropical areas is usually regarded as extreme due to the high temperatures, prolonged time-of-wetness, and high atmospheric contaminants (i.e. chlorides and  $\text{SO}_2$ ) and other factors such as rainfall, winds, etc. The salinity of aerosols may play an adverse effect in the formation of protective patina accelerating the process of atmospheric corrosion. In Panama, a country of two oceans, there have been some systematic studies of atmospheric corrosion of steels [2–5]. In some recent studies, we have focused on the determination of phase composition and other characteristics of steel corrosion products exposed to the tropical climate of Panama [6–12]. In this paper, we report the results of a five-year corrosion assessment of a low-carbon steel and a conventional weathering steel exposed to the Panamanian tropical atmosphere, as continuation of previous works [11, 12].

## 2 Materials and methods

The composition of the mild steel (A-36) and weathering steel (A-588) used in this study have been described elsewhere [11]. Coupons of 150 mm  $\times$  100 mm were used for atmospheric exposure. The samples were exposed at 45° to the horizontal at Tocumen site and at 30° in Sherman. After blasting, cleaning and degreasing with acetone, they were exposed to environment on inert racks for more than five years (January 2007–September 2012). Coupons were exposed at two different test sites, one an urban site in Panama City: 5 km from the shoreline of the Pacific Ocean, and another in the marine environment of Fort Sherman in the Caribbean coast of Panama; namely, Fort Sherman Coastal site: 600 m from coastline [11].

The corrosivity classification for each test station, based on environmental data (time of wetness, chloride and  $\text{SO}_2$  deposition rates), per ISO 9223, are  $\text{S}_1\text{P}_0\tau_4$  and  $\text{S}_1\text{P}_0\tau_5$  for Tocumen and Sherman Coastal sites, respectively [12].

In both sites,  $\text{SO}_2$  deposition is not an important parameter in terms of the aggressiveness of the test sites, whereas the TOW was in the highest categories ( $\tau_4$  and  $\tau_5$ ), according to ISO 9223 standard [13]. The  $\text{Cl}^-$  deposits were observed in higher amount compared to the  $\text{SO}_2$ , being slightly higher in Sherman Coastal test site. Based on the measured values of  $\text{SO}_2$  and  $\text{Cl}^-$ , Tocumen site can be classified as C3 with reference to ISO 9223-2012 classification and Sherman Coastal site as C4. After exposure, corrosion rates (corrosion penetration  $p$ ) were calculated from weight losses according to standard methods [14]. Corrosion products were separated mechanically before determining corrosion rates. Bulk rust, herein called non-adherent rust layer, was collected from the skyward and earthward faces. The adherent rust layers were carefully scrapped from the specimen using a spatula.

The attenuated total reflection Fourier transform infrared (ATR-FTIR) spectra of rusts were recorded in the 4000–400  $\text{cm}^{-1}$  range on a Bruker ALPHA /Platinum-ATR single

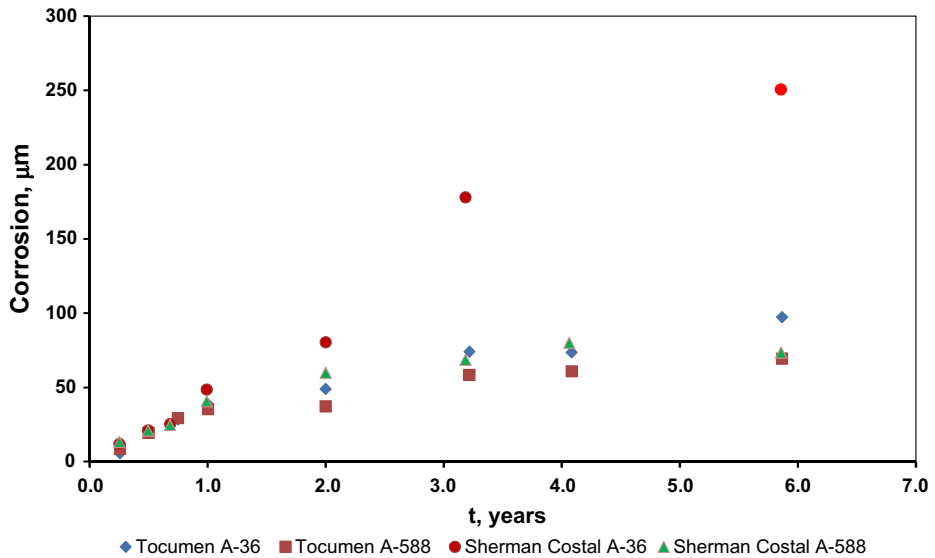


**Fig. 1** Atmospheric corrosion rate for steels as a function of exposure time

reflection diamond ATR module. Twenty-four scans with a  $4\text{ cm}^{-1}$  resolution were accumulated for each sample. Mössbauer spectra (MS) were recorded using a conventional spectrometer of constant acceleration with a  $^{57}\text{Co}(\text{Rh})$  source of nominal activity of 10 mCi (370 MBq). A closed-cycle cryostat (CCS 850 Janis) was employed for low temperature measurements. Calibrations were done with a standard  $\alpha$ -iron foil absorber at room temperature. The Mössbauer data were evaluated with the Recoil software (University of Ottawa, Canada) using Voigt base fitting.

### 3 Results and discussion

#### 3.1 Atmospheric corrosion kinetics

Figure 1 shows the variation in the corrosion ( $\mu\text{m}\cdot\text{y}^{-1}$ ) of both steels at the two test sites throughout the period of exposure. In all cases, an increase in the mass loss was observed, which tended to stabilize over time in all cases except for steel A-36 in the Coastal site. It should be noted that the reported rates of corrosion are the result of an average of the rates of both sides, the skyward and earthward faces. These corrosion rates are not necessarily the same, as established by differences in corrosion products.

The corrosion rates results obtained in the different steels at the Tocumen and Coastal stations are low or moderate. The fact of having smaller mass penetration (corrosion) after three years suggests that the A-588 steel exposed at Sherman site has a greater resistance to atmospheric corrosion when compared to A-36 steel. The estimated corrosion of a metal in each environment has been evaluated by means of the Passano exponential equation  $P = A \cdot t^n$  [15, 16], where P represents the corroded amount expressed as penetration corroded ( $\mu\text{m}$ ) or as weight loss, t is time in years, and A and n represent empirical constants. The results are consistent with the following:

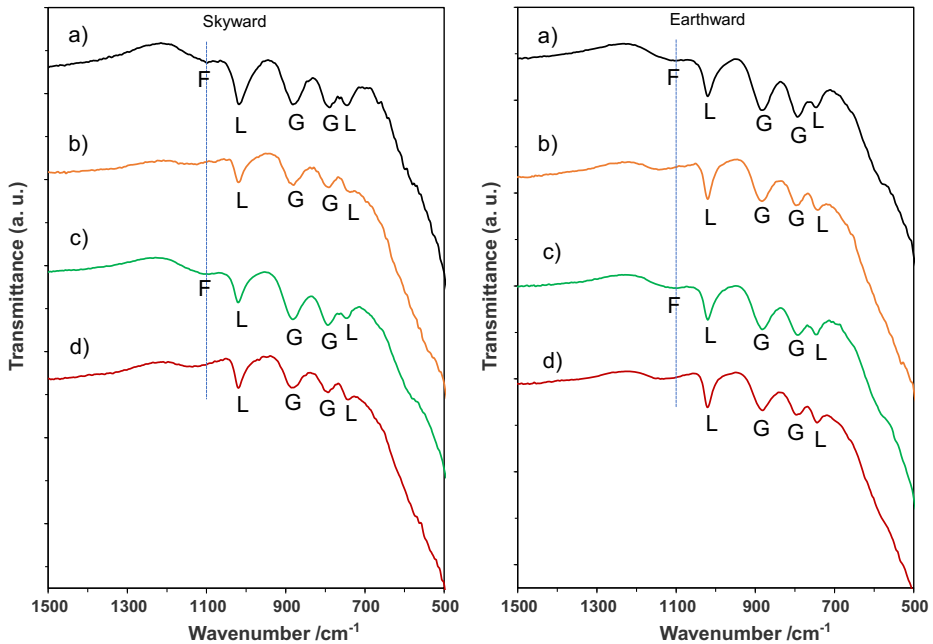


**Fig. 2** ATR-FTIR spectra of rusts formed at skyward and earthward faces of steel A-36 at **a** Tocumen site, **b** Sherman-Coastal site, and WS A-588 **c** Tocumen site, **d** Sherman-Coastal site (G-Goethite, L-Lepidocrocite, F-Feroxyhyte). The vertical dashed line corresponds to  $1100\text{ cm}^{-1}$

Tocumen station:

$$\text{A-36} \quad P = 28.2 t^{0.79 \pm 0.10} \quad \text{with } R^2 = 0.907 \quad (1)$$

$$\text{A-588} \quad P = 27.6 t^{0.64 \pm 0.07} \quad \text{with } R^2 = 0.927 \quad (2)$$

Sherman Coastal station:

$$\text{A-36} \quad P = 44.4 t^{1.02 \pm 0.05} \quad \text{with } R^2 = 0.986 \quad (3)$$

$$\text{A-588} \quad P = 33.2 t^{0.59 \pm 0.06} \quad \text{with } R^2 = 0.858 \quad (4)$$

The value of “*n*” confirms that the rust of A-36 mild carbon steel is not protective; as noticed previously [12], in the Coastal station linear behaviour was observed for steels A-36 instead of the expected parabolic behaviour. On the other hand, the “*n*” values greater than 0.5 obtained for the A-588 steel indicate that this steel produces more protective rusts, but still the protective rust layer is not completely consolidated. A closer value on “*n*” to 0.5 is required for all the corrosion products to remain on the metal surface providing a barrier to the passage of aggressive agents, and consequently, decreasing the corrosion rate.

The value of “*n*” depends on the metal concerned, the local atmosphere, and the exposure conditions. The fact that the protective patina has not fully developed (i.e. steady-state steel corrosion rates has not been reached) on the weathering steel in none of the test stations obviously has to do with the low atmospheric  $\text{SO}_2$  content. But it is also affected by the chloride levels of  $\text{Cl}^{-1}$   $11\text{--}30\text{ mg}\cdot\text{m}^{-2}/\text{d}$  (regardless of the proximity to the sea), and much more with the high time of wetness (TOW)  $55\text{--}67\%$  [12]. Hence, the exposure conditions cause the rust layer to be less protective.

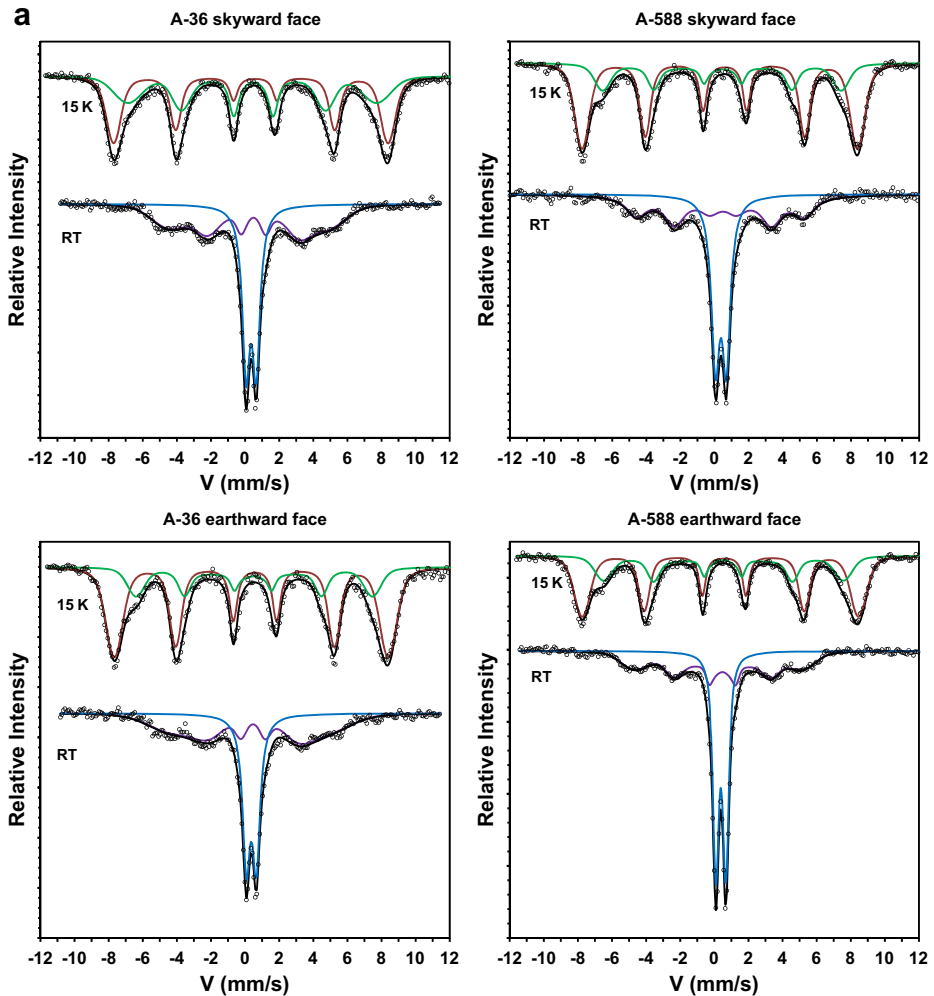


**Fig. 3** Mössbauer spectra at room temperature and 15 K of the non-adherent rust from **a** Tocumen site and **b** Sherman-Coastal site

### 3.2 ATR-FTIR characterization

The corrosion products of the non-adherent rust at the different test sites were analyzed using ATR-FTIR. Figure 2 shows the ATR-FTIR spectra of the corrosion products from skyward and earthward facing samples of mild and weathering steel. The OH bending bands at  $1019\text{ cm}^{-1}$  and  $742\text{ cm}^{-1}$  correspond to lepidocrocite ( $\gamma\text{-FeOOH}$ ), whereas the peaks at  $882\text{ cm}^{-1}$  and  $793\text{ cm}^{-1}$  are ascribed to goethite ( $\alpha\text{FeOOH}$ ). These bands appear in all spectra, including the non-adherent rust.

Two other salient features of the ATR-FTIR spectra were observed. The Sherman Coastal ATR-FTIR patterns show a broad, weak peak at around  $1130\text{ cm}^{-1}$ , expected for a O-H stretching absorption in lepidocrocite. On the other hand, the Tocumen samples exhibit

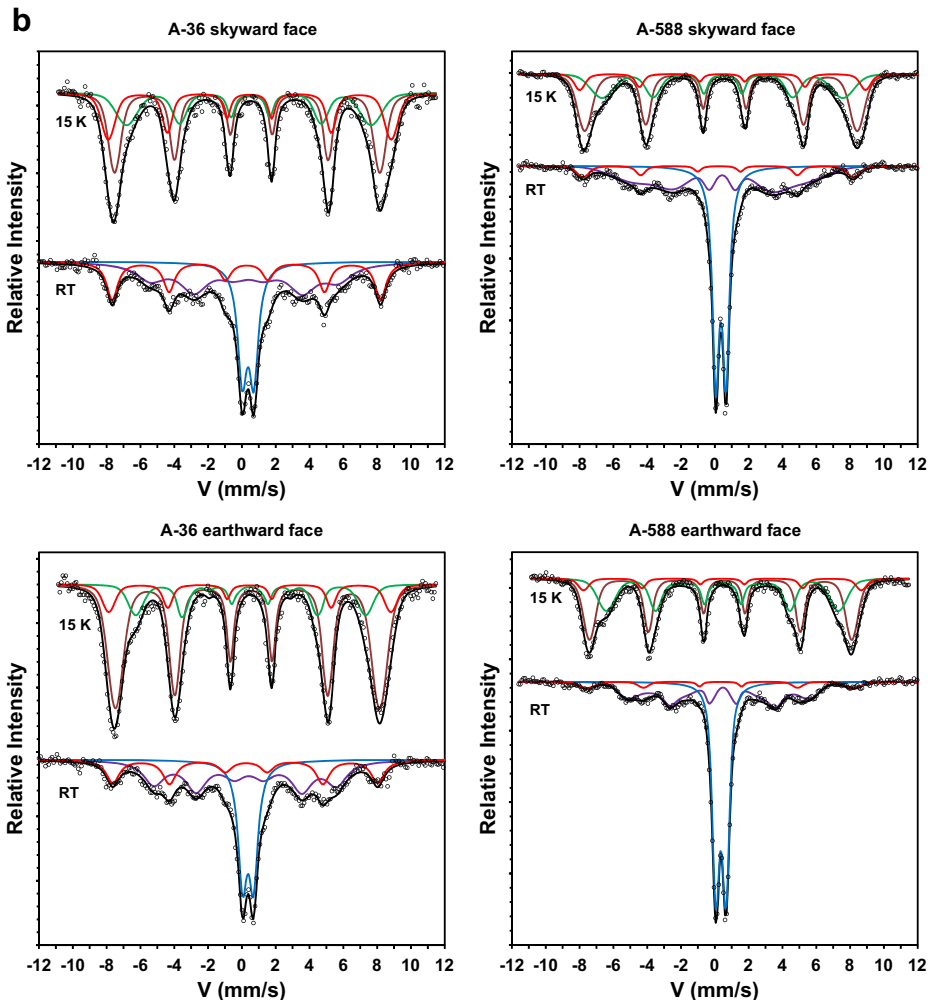


**Fig. 3** (continued)

a broad, but well defined absorption peak at  $1100\text{ cm}^{-1}$ , which is interpreted as a contribution of not so well crystallized feroxyhyte phase ( $\delta\text{-FeOOH}$ ) or a mixture of poorly crystalline lepidocrocite and feroxyhyte [17]. This phase, feroxyhyte, has been occasionally reported as a product of the early atmospheric corrosion of weathering steels [18–20]. Interestingly, the observed separation of the OH bending bands is only  $90\text{ cm}^{-1}$ , suggesting poorly crystallized goethite, as usually observed in corrosion products of steel.

### 3.3 Mössbauer analysis

Figure 3a and b show the Mössbauer spectra at room temperature and 15 K of the non-adherent rust. The RT Mössbauer spectra were fitted using two sextets (magnetic field distributions) and a paramagnetic doublet. The fitting parameters of the Mössbauer spectra

**Table 1** Mean Mössbauer parameters obtained from the fit of the spectra of corrosion products of steels exposed at Tocumen and Sherman sites

T K	Component	$\langle \delta \rangle$ mm/s	$\langle  B  \rangle$ T	$\langle \Delta \rangle / 2 < \epsilon >$ mm/s	Assignment
RT	QSD1	$0.37 \pm 0.02$	–	$0.60 \pm 0.02$	$\gamma$ -FeOOH + SPM $\alpha$ -FeOOH
	HFD1	$0.34 \pm 0.02$	$26.7 \pm 2.3$	$-0.25 \pm 0.02$	$\alpha$ -FeOOH (m)
	HFD2	$0.30 \pm 0.04$	$48.9 \pm 1.0$	$-0.03 \pm 0.02$	$\gamma$ -Fe <sub>2</sub> O <sub>3</sub>
15	HFD1	$0.46 \pm 0.01$	$51.9 \pm 0.3$	$0.02 \pm 0.02$	$\gamma$ -Fe <sub>2</sub> O <sub>3</sub>
	HFD2	$0.46 \pm 0.01$	$49.4 \pm 0.8$	$-0.24 \pm 0.02$	$\alpha$ -FeOOH
	HFD3	$0.48 \pm 0.03$	$41.2 \pm 2.7$	$0.00 \pm 0.05$	$\gamma$ -FeOOH

The values given represent averages and the errors are estimated from the scatter in the different measurements.

- $\langle \delta \rangle$ : average isomer shift with respect to  $\alpha$ -Fe
- $\langle |B| \rangle$ : average of the hyperfine magnetic field distribution
- $\langle \epsilon \rangle$ : average quadrupole shift
- $\langle \Delta \rangle$ : average quadrupole splitting

are presented in Table 1. The broad sextet of sample HFD1 has Mössbauer parameters that can be associated with goethite [21–23]. The appearance of the lines, due to a broad distribution with the average of the hyperfine magnetic field ranging from 27–32 T is indicative of the smaller particle size of this component in the rust. The incipient sextet HFD2, observed in spectra of rust of the steels exposed at Sherman site, has parameters similar to those of maghemite [21–23]. The paramagnetic doublet QSD1 is assigned unambiguously to (super)paramagnetic compounds in the rust layers (lepidocrocite, superparamagnetic goethite, and/or other oxides or oxyhydroxides).

The 15 K Mössbauer spectra for rust from steels collected at Tocumen site (Fig. 3a) show two components, whereas for the Sherman site (Fig. 3b) exhibit three components. The Mössbauer parameters are characteristic of maghemite, goethite and lepidocrocite. Sextet HFD1 attributed to maghemite in spectra of rust of the steels exposed at Sherman site, exhibiting a hyperfine field around 51.9 T, may have the contribution of another phase, ferroxhyte. This compound, detected in the ATR-FTIR spectra, has a hyperfine magnetic field of 52.5 T at low temperatures [22]. Nonetheless, the inclusion of an extra sextet in the fitting procedure did not result in improvements. It might be possible that it occurs in very small quantities, difficult to be detected with Mössbauer spectroscopy. It should be recalled that infrared techniques can detect trace amounts (1–2 %) of non-crystalline and not well crystallised phases, but Mössbauer requires more than ca. 5 %. The assignment to maghemite with a particle size distribution is therefore kept.

Table 2 summarizes the Mössbauer results obtained as relative abundance determined from the room temperature and 15 K data. From this table, it can be seen that, for both steels, lepidocrocite and goethite are the main corrosion products, followed by maghemite. It is interesting to note that the amounts of lepidocrocite over time tend to decrease, probably favoring the formation of goethite. At the same time, the quantities of coarse goethite increase. We have proposed [7] that this goethite has a certain degree of protective ability against further atmospheric corrosion. However, the performance of the protection is

**Table 2** Estimated relative concentrations (%) in the corrosion products after exposure at tests sites

Exposure time	Type of Steel	Exposure site	$\alpha$ -FeOOH(m) <sup>1</sup>	$\alpha$ -FeOOH(s) <sup>2</sup>	Total		$\gamma$ -FeOOH	$\gamma$ -Fe <sub>2</sub> O <sub>3</sub>	Reference
					$\alpha$ -FeOOH	$\gamma$ -FeOOH			
3 months	A-36	Tocumen	13.4	37.1	50.5	49.5	–	23	
		Sherman-Coastal	35.0	15.7	50.7	42.9	6.4		
		A-588	Tocumen	28.4	25.0	53.4	46.6	–	
	A-588	Sherman-Coastal	29.4	22.4	51.8	42.8	5.4		
		A-36	Tocumen	23.6	41.6	65.2	34.8	–	24
			Sherman-Coastal	25.3	41.1	66.4	33.6	–	
6 months	A-36	Tocumen	23.6	41.6	65.2	34.8	–	24	
		Sherman-Coastal	25.3	41.1	66.4	33.6	–		
		A-588	Tocumen	38.0	27.7	65.7	34.3	–	
	A-588	Sherman-Coastal	43.3	17.2	60.5	39.5	–		
		A-36	Tocumen	43.8	23.0	66.8	33.2	–	24
			Sherman-Coastal	46.7	7.5	54.2	37.9	7.9	
1 year	A-36	Tocumen	43.8	23.0	66.8	33.2	–	24	
		Sherman-Coastal	46.7	7.5	54.2	37.9	7.9		
		A-588	Tocumen	48.3	15.0	63.3	36.7	–	
	A-588	Sherman-Coastal	23.6	20.8	44.4	40.6	15.0		
		A-36	Tocumen	51.6	–	51.6	48.4	–	This work
			Sherman-Coastal	44.6	–	44.6	27.6	27.8	
5 year Skyward	A-36	Tocumen	51.6	–	51.6	48.4	–	This work	
		Sherman-Coastal	44.6	–	44.6	27.6	27.8		
		A-588	Tocumen	45.9	22.8	68.7	31.3	–	
	A-588	Sherman-Coastal	41.9	12.7	54.6	33.3	12.1		
		A-36	Tocumen	54.6	15.2	69.8	30.2	–	This work
			Sherman-Coastal	47.8	20.6	68.4	18.6	13.0	
5 year Earthward	A-36	Tocumen	54.6	15.2	69.8	30.2	–	This work	
		Sherman-Coastal	47.8	20.6	68.4	18.6	13.0		
		A-588	Tocumen	48.8	14.7	63.5	36.5	–	
	A-588	Sherman-Coastal	37.5	17.1	54.6	33.3	12.2		

<sup>1</sup> $\alpha$ -FeOOH(m): magnetic goethite (>15 nm) exhibiting magnetic sextet at 298 K

<sup>2</sup> $\alpha$ -FeOOH(s): superparamagnetic goethite (<15 nm) exhibiting superparamagnetic doublet at 298 K and magnetic sextet at low temperatures (e.g. 80 K or below)

hindered by the morphology of rust, and the presence of pores and cracks. Marco et al. [23] pointed out that the size of the goethite particles might increase via nucleation on preexistent goethite. The layer structure in rust is loose, not providing enough protection.

Only in Sherman-Coastal test site maghemite is formed, which correlates with the observed rate of corrosion for both steels, and explain the higher corrosion observed for steel A-36 in Sherman-Coastal site. The presence of maghemite reduces drastically the rust protection, which is reason for the corrosion rate to be higher in the coastal season than in

Tocumen, mainly for the mild steel A-36. Chloride levels and TOW on average are slightly higher at the Sherman-Coastal station, enough to promote the formation of this corrosion pernicious phase. The ratio ( $\alpha_m/\gamma^*$ ), where  $\alpha$  and  $\gamma^*$  are the mass ratio of crystalline  $\alpha$ -FeOOH to the total of  $\gamma$ -FeOOH,  $\beta$ -FeOOH and spinel-type iron oxide, respectively, is used for defining a Protective Ability Index (PAI) of the rust layer [24, 25]. The rust obtained for over five years' exposure under mild tropical conditions is non-protective, inactive and cause moderate corrosion rates; the protective layer has not been formed.

For both type of steels, the room temperature Mössbauer spectra of adherent rust separated from skyward faces of samples are very similar to those obtained for the non-adherent rust. In order to study the nature of this innermost layer, transmission Mössbauer is probably not the most suitable method, and a surface technique should be used instead (e.g. CEMS, DCEMS, etc.).

## 4 Conclusion

The atmospheric corrosion behaviour of samples of carbon steel A-36 and conventional weathering steels A-588 proceeded according to the well-known bilogarithmic law for weight loss, but in the Sherman-Coastal test site a linear behaviour was observed for steels A-36. The type of steel, chloride content and relative humidity have an important influence on the steel corrosion. The corrosion products which form on steel A-36 and steel A-588, under mild to moderate weather conditions and contamination, have not developed a protective rust layer. Even though the difference in corrosion of steels at the various sites with mild conditions was small, the weathering steels A-588 has a little better protection after the period of study.

The main constituents of the rust formed in the skyward and earthward faces in the studied tropical environment are goethite and lepidocrocite. In the early stages of atmospheric corrosion, the formation of lepidocrocite is predominant, over time tend to decrease favoring the formation of goethite. The Sherman-Coastal samples also show the presence of small amounts of maghemite, as shown by Mössbauer spectra. This result explains the higher corrosivity observed in this test station for mild steel A-36, in which rust is obtained with greater amount of maghemite. Ferroxihite is also detected in the ATR-FTIR spectra for Tocumen samples.

**Acknowledgments** The authors thank SENACYT of Panama for the award through the National Research System (SNI).

## References

1. Pourbaix, M.: *Tournée d'été de la CEFA, Corrosion atmosphérique des aciers patinables*. Rapport Technique 217, Ed. CEBELCOR, Bruxelles, pp. 18–32 (1973)
2. Alexander, A.L., Forgeson, B.W., Mumdt, H.W., Southwell, C.R., Thompson, S.J.: *NRL Report 4929 corrosion of metals in tropical environments, part-1 test methods used and result obtained for pure metals and a structural steel*. Washington D.C. (1957)
3. Southwell, C.R., Forgeson, B.W., Alexander, A.L.: *NRL Report 5002, corrosion of metals in tropical environments, part-2 atmospheric corrosion of ten structural steels*. Washington D.C. (1957)
4. Morcillo, M., Almeida, E., Rosales, B., Uruchurtu, J., Marrocos, M.: *Corrosión y Protección de Metales en las Atmósferas de Iberoamérica. Parte I: Mapas de Iberoamérica de Corrosividad Atmosférica (Red Temática MICAT XV.1/CYTED)*. CYTED, Madrid (1999)

5. Morcillo, M., Almeida, E., Fragata, F., Panossian, Z.: Corrosión y Protección de Metales en las Atmósferas de Iberoamérica. Parte II: Protección Anticorrosiva de Metales en las Atmósferas de Iberoamérica (Red Temática PATINA, XV.D/CYTED). CYTED, Madrid (2002)
6. Jaén, J.A., Fernández, B.: Mössbauer spectroscopy study of steel corrosion in a tropical marine atmosphere. *Electrochem. Acta* **34**, 885–886 (1989)
7. Jaén, J.A., Sánchez de Villalaz, M., de Araque, L., de Bósquez, A.: Kinetics and structural studies of the atmospheric corrosion of carbon steels in Panama. *Hyperfine Interact.* **110**, 93–99 (1997)
8. Jaén, J.A., Sánchez de Villalaz, M., de Araque, L., de Bósquez, A.: Study of the corrosion products formed on carbon steels in the tropical atmosphere of Panama. *Rev. Metal. Madrid Vol. Extr.* 32–37 (2003)
9. Jaén, J.A., Garibaldi, G.: Estudio del Efecto Estacional sobre la Corrosión Atmosférica Inicial de Aceros de Bajo Carbono en la Ciudad de Panamá. *Tecnociencia* **6**(2), 137–152 (2004)
10. Jaén, J.A., Araque, L.: de: Caracterización de los Productos de Corrosión de Aceros al Carbono en el Clima Tropical Marino de Sherman (Provincia de Colón, Panamá). *Tecnociencia* **8**(1), 49–63 (2006)
11. Jaén, J.A., Muñoz, A., Justavino, J., Hernández, C.: Characterization of initial atmospheric corrosion of conventional weathering steels and a mild steel in a tropical atmosphere. *Hyperfine Interact.* **192**(1), 51–59 (2009)
12. Jaén, J.A., Iglesias, J., Hernández, C.: Analysis of short-term steel corrosion products formed in tropical marine environments of Panama. *Int. J. Corrosion* **2012**, Article ID 162729, 11 pages (2012). doi:[10.1155/2012/162729](https://doi.org/10.1155/2012/162729)
13. ISO 9223:2012: Corrosion of metals and alloys, Corrosivity of atmospheres. Classification, 2012. ISO 9223, Corrosion of Metal and Alloys—Classification of Corrosivity of Atmospheres, International Standards Organization, Geneva, Switzerland (2012)
14. ISO 9226:2012: Corrosivity of atmospheres—determination of corrosion rate of standard specimens for the evaluation of corrosivity. International Standards Organization, Geneva, Switzerland (2012)
15. Passano, R.F.: Proceedings of the symposium on the outdoor weathering of metals and metallic coating. Philadelphia (1934)
16. Pourbaix, M.: The linear bilogarithmic law for atmospheric corrosion. In: Aylor, W.H. (ed.) *Atmospheric Corrosion*, pp. 107–121. Wiley, New York (1982)
17. Raman, A., Kuban, B., Razvan, A.: The application of infrared spectroscopy to the study of atmospheric rust systems—I. Standard spectra and illustrative applications to identify rust phases in natural atmospheric corrosion products. *Corros. Sci.* **32**(12), 1295–1306 (1991)
18. De Souza, P.A. Jr., Demacêdo, M.C.S., De Queiro, R.S., Klingelhöfer, G.K.: Atmospheric corrosion investigation in industrial, marine and rural environments in South-East Brazil. *Hyperfine Interact.* **139/140**, 183–191 (2002)
19. Ocampo, C.L.M., Mattos, O.R., Margarit-Mattos, I.C.P., Fabris, J.D., Pereira, M.C., Rechenberg, H.R., de Faria, D.L.A.: Influence of Cu and Ni on the morphology and composition of the rust layer of steels exposed to industrial environment. *Hyperfine Interact.* **167**, 739–746 (2006)
20. Li, Q.X., Wang, Z.Y., Han, W., Han, E.H.: Characterization of the rust formed on weathering steel exposed to Qinghai salt lake atmosphere. *Corros. Sci.* **50**, 365–371 (2008)
21. Murad, E., Johnston, J.H.: Iron oxides and oxyhydroxides. In: Long, G.J., Murata, T. (eds.) *Mössbauer Spectroscopy Applied to Inorganic Chemistry*, pp. 507–582. Plenum Press, New York (2000)
22. Oh, S.J., Cook, D.C., Townsend, H.E.: Characterization of iron oxides commonly formed as corrosion products on steel. *Hyperfine Interact.* **112**, 59–65 (1998)
23. Marco, J.F., Gracia, M., Gancedo, J.R., Martín-Luengo, M.A., Joseph, G.: Characterization of the corrosion products formed on carbon steel after exposure to the open atmosphere in the Antarctic and Easter Island. *Corros. Sci.* **42**, 753–771 (2000)
24. Cook, D.C.: Spectroscopic identification of protective and non-protective corrosion coatings on steel structures in marine environments. *Corros. Sci.* **47**(10), 2550–2570 (2005)
25. Kamimura, T., Hara, S., Miyuki, H., Yamashita, M., Uchida, H.: Composition and protective ability of rust layer formed on weathering steel exposed to various environments. *Corros. Sci.* **48**, 2799–2812 (2006)